Semi-solid near-net shape rheocasting of heat treatable wrought aluminum alloys

U. A. CURLE

Materials Science and Manufacturing, Council for Scientific and Industrial Research, Pretoria, South Africa

Abstract: Flexibility of the CSIR-RCS, induction stirring with simultaneous air cooling process, in combination with high pressure die casting is successfully demonstrated by semi-solid rheocasting of plates performed on commercial 2024, 6082 and 7075 wrought aluminum alloys. Tensile properties were measured for the above mentioned rheocast wrought aluminum alloys in the T6 condition. The results showed that tensile properties were close to or even in some cases exceeded the minimum specifications. The yield strength and elongation of rheocast 2024-T6 exceeded the minimum requirements of the wrought alloy in the T6 condition but the ultimate tensile strength achieved only 90% of the specification because the Mg content of the starting alloy was below the commercial alloy specification. The strengths of rheocast 6082-T6 exceeded all of the wrought alloy T6 strength targets but the elongation only managed 36% of the required minimum due to porosity, caused by incipient melting during solution heat treatment, and the presence of fine intermetallic needles in the eutectic. The yield strength of rheocast 7075 exceeded the required one and the ultimate tensile strength also managed 97% of the specification; while the elongation only reached 46% of the minimum requirement also due to incipient melting porosity caused during the solution heat treatment process.
Key words: high pressure die casting (HPDC); aluminum alloys; as-cast condition; T6 treatment; incipient melting

1 Introduction

Near-net shape casting of components from wrought alloys is a challenge due to hot tearing[1−3]. Although an opportunity arose with the advent of semi-solid processing, it still remains largely out of reach on a meaningful commercial scale[2]. Much attention has been given in recent years to the thixocasting route of different wrought alloys in which semi-solid metal (SSM) is created by partial melting of solid feedstock material before shaping[3−19].

The rheocasting route for wrought alloys where SSM is created from the liquid state has received considerably less attention. Although there are indications that semi-solid state wrought aluminum alloys can be prepared[20−21], there has been limited demonstration of actual shape rheocasting[2, 22−24] or rheoforging[25−27].

The single coil version of the CSIR-RCS in conjunction with a high pressure die casting has been used, in the past, to demonstrate casting of Al-Si casting alloys[28−31] as well as Al-Cu-(Ag) casting alloys[32].

It has been suggested before that the future of SSM casting will be in the area of wrought alloy compositions[33] and therefore the aim here is to show that shape rheocasting of wrought aluminum alloys is practical with the CSIR-RCS while also relating the tensile properties obtained to microstructural features. The current investigation did not attempt to optimize the heat treatment for the SSM wrought alloy structures.

2 Experimental

Commercial wrought alloys 2024, 6082 and 7075 were used for rheo-processing and high pressure die casting (HPDC) of plates having dimensions of 100 mm×55 mm×6 mm. Fig.1 shows the whole casting including the biscuit and the runner.

A batch of each wrought alloy was melted in a 20 kg resistance heated tilting furnace and degassed with argon. A sample was poured and cooled to analyze the chemical composition by optical emission spectroscopy (Thermo Quantris OES). Table 1 shows the chemical composition obtained for each of the wrought alloys.
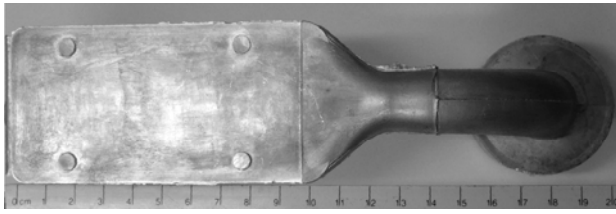
Fig.1 Example of rheocast wrought alloy plates including runner and biscuit

Table 1 Chemical compositions of commercial wrought alloys used in this study (mass fraction, %)

Alloy	Zn	Mg	Cu	Si	Mn	Cr	Fe
2024	0.06	1.07	4.14	0.07	0.60	0.01	0.15
Specific min.	−	1.20	3.80	−	0.30	−	−
Specific max.	0.25	1.80	4.90	0.50	0.90	0.10	0.50
6082	0.10	0.89	0.05	0.92	0.49	0.03	0.32
Specific min.	−	0.60	−	0.70	0.40	−	−
Specific max.	0.20	1.20	0.10	1.30	1.00	0.25	0.50
7075	5.79	2.38	1.43	0.23	0.14	0.16	0.21
Specific min.	5.10	2.10	1.20	−	−	0.18	−
Specific max.	6.10	2.90	2.00	0.40	0.30	0.28	0.50

Specification limits from Refs.[34−36].

Thermodynamic properties of each alloy were then calculated with an aluminum thermodynamic database (ProCast 2009.1) from the specific OES compositions given in Table 1. Table 2 summarizes the calculated thermodynamic properties and deduced rheocasting parameters. A pouring temperature of approximately 40 °C above the liquidus (the pouring temperature sensitivity has not yet been established) and a SSM processing temperature corresponding to a solid fraction of 30% were used from experience with the system.

The sequence for casting was as follows. Liquid metal was poured from the tilting furnace into the

Table 2 Calculated thermodynamic properties and deduced rheo-processing parameters for wrought alloys used

Alloy	Temperature/°C			
	Liquidus	Solidus	Pouring	SSM
2024	644	500	680	636.5
6082	649	553	690	645.3
7075	635	486	670	622.8

stainless steel processing cup (about 400 g) which was then manually transferred to a single coil version of the CSIR-RCS (induction stirring with simultaneous forced air cooling[37]) where processing starts when the cup enters the coil. The semi-solid temperature of the material in the cup was measured by a thermocouple. Processing stopped after the thermocouple signal reached the preset SSM temperature. At this point, the cup was ejected from the coil and manually transferred to the HPDC machine (LK DCC130). The injection shot was manually triggered when the SSM billet was in the shot sleeve. The piston followed the set computer controlled injection velocity profile which was kept the same for the different wrought alloys.

Rheocast plates, from each wrought composition in the as-cast (F) condition, were selected and heat treated to the T6 condition with parameters shown in Table 3. Subsize rectangular tensile test specimens were machined from the plates according to ASTM standards[39] and the tensile properties were evaluated (Instron Model 1342).

Table 3 T6 heat treatment parameters for rheocast wrought alloys with conventional artificial aging temperatures and times used[38]

Alloy	Solution treatment		Artificial aging	
	Temperature/°C	Time/h	Temperature/°C	Time/h
2024	480	14	190	12
6082	540	2	177	10
7075	475	4	120	24

An optical microscope (Leica DMI5000 M) equipped with a camera (Leica DFC480) and imaging software (Image–Pro MC v6.0) revealed the F and T6 condition microstructures after polishing and etching with 0.5% HF.

3 Results and discussion

Plates of wrought aluminum alloys 2024, 6082 and 7075 were successfully rheocast with the CSIR-RCS without evidence of hot tearing. The surface finish on all the rheocast alloy plates was smooth and bright.

Fig.2 shows the proeutectic alpha globules, in the aluminum alloy 2024, which are reasonably spherical although have a large size distribution. The eutectic areas are noticeably coarse in the F condition, while in the T6 condition it seems as if the eutectic areas have increased after even light etching. This effect is assumed to be related to copper diffusion from the concentration on the grain boundaries and eutectic areas into the grains.

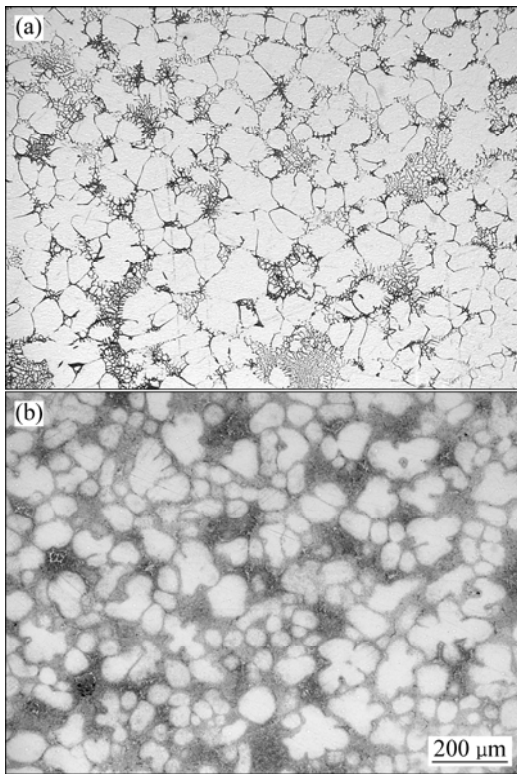Fig.3 shows the microstructures in the case of the

Fig.2 Optical micrographs of rheocast aluminum alloy 2024 in F condition (a) and T6 condition (b)
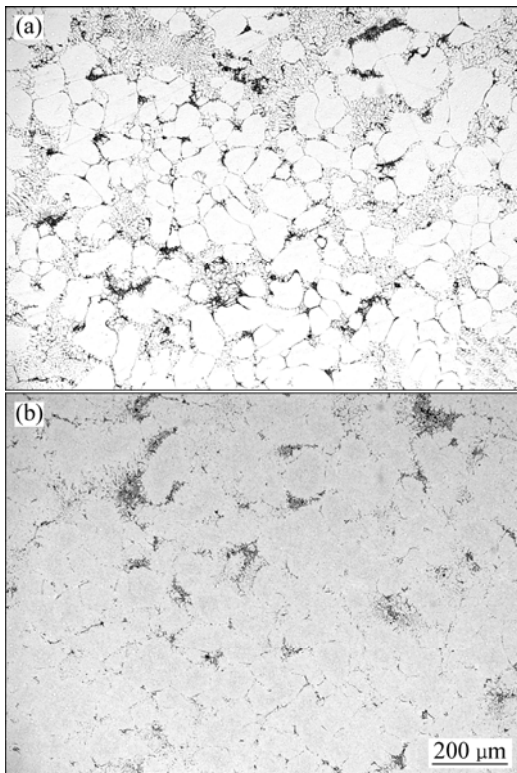

Fig.3 Optical micrographs of rheocast aluminum alloy 6082 in F condition (a) and T6 condition (b)

aluminum alloy 6082 which has similar features to the aluminum alloy 2024 in the F condition. In the T6

condition, on the other hand, it seems that the eutectic grain boundaries have disappeared while coarse eutectic areas remain pronounced.

Fig.4 shows the microstructures of the rheocast aluminum alloy 7075. Again very similar features to both of the other two rheocast wrought alloys used in this investigation are observed. It will be seen later that the dark spots in the eutectic areas of Fig.4(a) are a consequence of a phase that is formed during solidification.
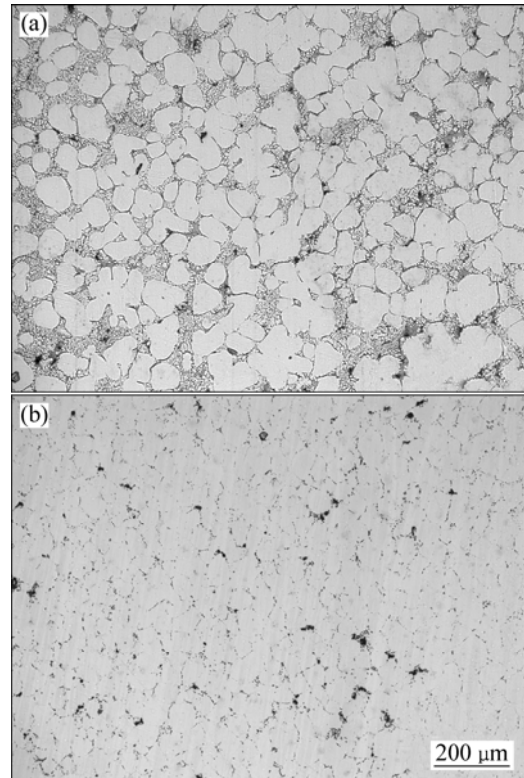

Fig.4 Optical micrographs of rheocast aluminum alloy 7075 in F condition (a) and T6 condition (b)

A final note concerning the F condition grain structures is that the actual size and shape of the proeutectic globules are not important for the moment because the first challenge is to produce sound near-net shape wrought aluminum alloy rheocastings. A phenomenon that was identified in all the alloy castings was surface liquid segregation which has been addressed, as well as corrosion[40−41].

The tensile property results of all the rheocast aluminum wrought alloys in the T6 condition are given in Table 4. It is shown that all the yield strengths of rheocast wrought alloys exceeded the minimum yield strength specification.

The ultimate tensile strength of 2024-T6 reached 90% of the required minimum specification. Table 1 shows that the Mg content of the starting alloy is well below the minimum chemical specification and is a

Table 4 Tensile properties of rheocast wrought alloys in T6 condition

Alloy	YS/MPa	UTS/MPa	Elongation/%
2024 T6	351	385	5.1
Specific min.	345	427	5.0
6082 T6	341	365	3.6
Specific min.	260	310	10.0
7075 T6	467	513	3.2
Specific min.	455	531	7.0

Minimum tensile requirements from Refs.[34−36].

necessary element for precipitation strengthening[42]. The ultimate tensile strength of 6082-T6 rheocast alloy well exceeded the requirement with complete dissolution of Mg-Si phase at the relatively high temperature. The ultimate tensile strength of 7075-T6 rheocast alloy reached 97% of the minimum requirement most likely due to a short solution heat treatment time.

　　Full heat treatment procedures for each of these rheocast wrought alloys have not been optimized yet in terms of solution heat treatment times and temperatures for this manufacturing method. The point here is that very good yield strength and ultimate tensile strength results have been achieved in the first attempt.

　　The main concern is paid on the elongation results in Table 4. Rheocast 2024-T6 achieved the wrought alloy T6 specified requirement while rheocast 6082 T6 only 36% and rheocast 7075-T6 46% of their respective specified requirements.

　　Fig.5 shows that porosity (black dots) is the root cause of the poor elongation results in the case of rheocast 7075-T6 while in rheocast 6082-T6 needles (β-Al$_5$FeSi) also lead to the embrittlement effect[43]. In rheocast 2024-T6, only small pores are formed which accounts for its elongation result. It can be seen that the pores are associated with the eutectic areas in all the rheocast alloys in the T6 condition. Fig.2(b), Fig.3(b) and Fig.4(b) indicate on a larger scale the distribution of the pores for each of the rheocast wrought alloys in the T6 condition.

　　Fig.6 shows again the eutectic areas of each rheocast wrought alloy in the F condition. Interestingly, it is seen that there are fine dendritic phases present in the 2024 and 7075. Not only are there finely distributed black pin-head dots seen in the 6082 but also the needles are already present in the F condition. The eutectic areas were the last liquid to solidify so these dendritic phases must have a low melting point.

　　In comparison of the eutectic areas of the F condition and the T6 condition for each alloy, it is shown that the location of the porosity in the T6 condition
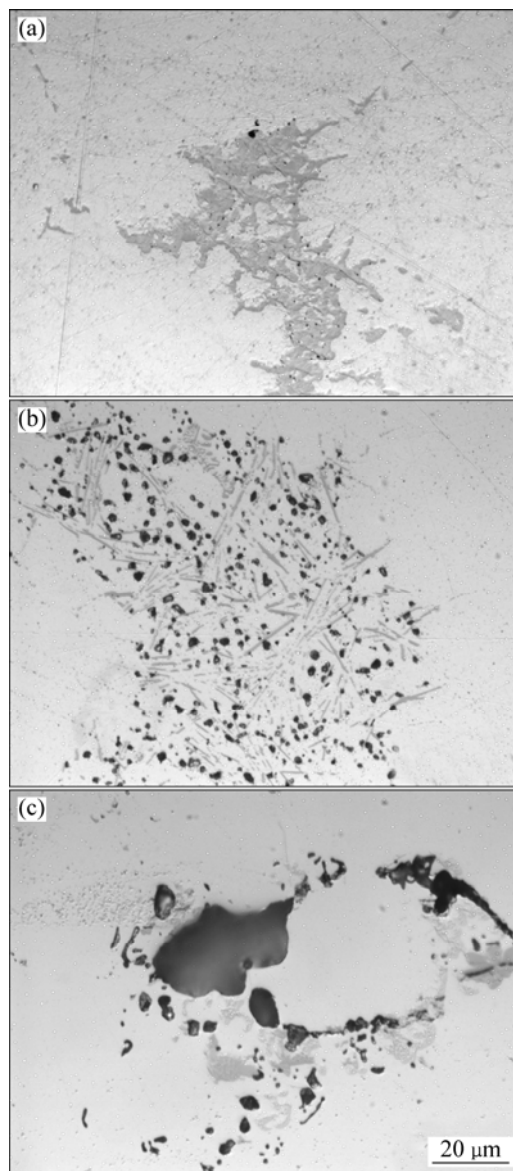

Fig.5 Optical micrographs of eutectic areas in rheocast aluminum 2024 (a), 6082 (b) and 7075 (c) in T6 condition (All unetched)

corresponds to the location of the dendritic phases in the case of rheocast alloys 2024 and 7075 and the pin-head pots of 6082, all in the F condition. Therefore, it is reasonable to assume that incipient melting of these low melting point phases occurred during the solution heat treatment.

　　The next step would be to identify the composition of each of these phases in order to optimize the heat treatment procedure for each of these rheocast wrought aluminum alloys. One option is to determine the melting points of these phases with differential scanning calorimetry (DSC) and work out a two step solution heat treatment procedure in order to still achieve the required strengths while more importantly achieve the minimum elongation requirements.
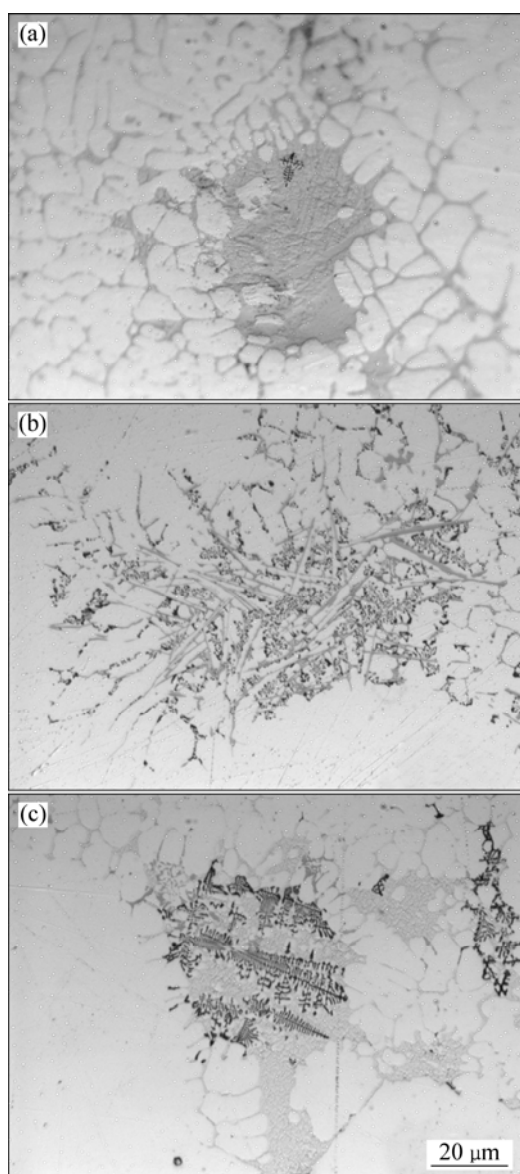
Fig.6 Optical micrographs of eutectic areas in rheocast aluminum 2024 (a), 6082 (b) and 7075 (c) in F condition (All unetched)

4 Conclusions

1) Semi-solid near-net shape rheocasting of heat treatable wrought aluminum 2024, 6082 and 7075 alloys are successful with the CSIR-RCS and high pressure die casting.

2) No evidence of hot tearing is observed. The grain structures show relatively spherical proeutectic alpha aluminum grains with areas of eutectic between grains.

3) Tensile properties reveal that all 0.2% offset yield strengths of the rheocast wrought aluminum alloys achieve the minimum specifications in the T6 condition.

4) Ultimate tensile strengths results in each case are close to the minimum required specification. Rheocast 6082-T6 far exceeds the requirement while rheocast 2024-T6 achieves 90% and rheocast 7075-T6 reaches 97% of the minimum specification. These results can be bettered by optimizing the solution heat treatment procedure.

5) Elongation results are poor because of porosity in the eutectic for rheocast 6082-T6 and rheocast 7075-T6 while rheocast 2024-T6 achieves the minimum requirement with the least porosity.

6) The observed porosity is caused by incipient melting during solution heat treatment.

References

[1] STALEY J T Jr, APELIAN D. Vacuum die-casting of wrought 7050 aluminum alloy [C]//Materials Solutions Conference. Indianapolis, IN, 2001: 290−297.

[2] LANGLAIS J, ANDRADE N, LEMIEUX A, CHEN X G, BUCHER L. The semi-solid forming of an improved AA6061 wrought aluminum alloy composition [J]. Diffusion and Defect Data Pt.B: Solid State Phenomena, 2008, 141/142/143: 511−516.

[3] OH S I, KANG B M, LEE S Y. Defects, microstructures and mechanical properties of thixoformed aluminum suspension parts for electric vehicle [C]//7th International Conference on Semi-Solid Processing of Alloys and Composites. Tsukuba, Japan, 2002: 725−730.

[4] KOPP R, WINNING G, KALLWEIT J, KNISSEL H, GABATHULER J P, QUAST R. Comparison of thixocasting and thixoforging using a unique demonstrator part [C]//6th International Conference on Semi-Solid Processing of Alloys and Composites. Turin, Italy, 2000: 687−691.

[5] CHAYONG S, KAPRANOS P, ATKINSON H V. Semi-solid processing of aluminium 7075 [C]//6th International Conference on Semi-Solid Processing of Alloys and Composites. Turin, Italy, 2000: 649−654.

[6] TAUSIG G. Assessment of aluminium feedstock materials for use in thixoforming [C]//6th International Conference on Semi-Solid Processing of Alloys and Composites. Turin, Italy, 2000: 489−494.

[7] GULLO G C, STAINHOFF K, UGGOWITZER P J. Microstructural changes during reheating of semi-solid alloy AA6082, modified with barium [C]//6th International Conference on Semi-Solid Processing of Alloys and Composites. Turin, Italy, 2000: 367−372.

[8] LIU D, ATKINSON H V, KAPRANOS P, JONES H. Effect of heat treatment on structure and properties of thixoformed wrought alloy 2014 [C]//7th International Conference on Semi-Solid Processing of Alloys and Composites. Tsukuba, Japan, 2002: 311−316.

[9] YANG G, TAUSIG G, XIA K. Equal channel angular deformation of a semisolid aluminum alloy 6082 [C]//7th International Conference on Semi-Solid Processing of Alloys and Composites. Tsukuba, Japan, 2002: 185−190.

[10] GOVENDER G. Semi-solid forming of 7075 aluminum alloys [C]//7th International Conference of Semi-Solid Processing of Alloys and Composites. Tsukuba, Japan, 2002: 179−184.

[11] KAPRANOS P, ATKINSON H V. Thixoforming 2014, 6082, 7010 and 7075 aluminium wrought alloys [C]//7th International Conference on Semi-Solid Processing of Alloys and Composites. Tsukuba, Japan, 2002: 167−172.

[12] JIRATTITICHAROEAN W, JONES H, ATKINSON H V, TODD I, KAPRANOS P. Thixoforming of aluminium 7xxx alloys produced using a cooling slope [C]//8th International Conference on Semi-Solid Processing of Alloys and Composites. Limassol, Cyprus,

2004: Unpresented Paper 08.

[13] AZPILGAIN Z, HURTADO I, BASTERRECHEA G, GANDARIAS E, GONI J, EGUIEABAL P, LAKEHAL M, SARRIES I, LANDA I, WIELANEK L. Development of aluminium alloys for the thixoforming process [C]//8th International Conference on Semi-Solid Processing of Alloys and Composites. Limassol, Cyprus, 2004: Paper 23−4.

[14] CHAYONG S, ATKINSON H V, KAPRANOS P. Thixoforming 7075 aluminium alloys [J]. Materials Science and Engineering A, 2005, 390(1/2): 3−12.

[15] YOON Y O, JO H H, LEE J K, JANG D I, KIM S K. Development of thixoextrusion process for 7000 series Al wrought alloys [J]. Diffusion and Defect Data Pt.B: Solid State Phenomena, 2006, 116/117: 771−774.

[16] VANEETVELD G, RASSILI A, LECOMTE-BECKERS J, ATKINSON H V. Thixoforging of 7075 aluminium alloys at high solid fraction [J]. Diffusion and Defect Data Pt.B: Solid State Phenomena, 2006, 116/117: 762−765.

[17] AZPILGAIN Z, HURTADO I, ORTUBAY R, LANDA I, ATXA J. Semisolid forging of 7000 series aluminum alloys [J]. Diffusion and Defect Data Pt.B: Solid State Phenomena, 2006, 116/117: 758−761.

[18] VANEETVELD G, RASSILI A, PIERRET J C, LECOMTE-BECKERS J. Improvement in thixoforging of 7075 aluminium alloys at high solid fraction [J]. Diffusion and Defect Data Pt.B: Solid State Phenomena, 2008, 141/142/143: 707−712.

[19] BIROL Y. Thixoforging experiments with 6082 extrusion feedstock [J]. Journal of Alloys and Compounds, 2008, 455(1/2): 178−185.

[20] OH S W, KANG C G, KIM B M. Grain size control of wrought aluminum alloy for rheology forging by electromagnetic stirring and its mechanical properties [J]. Diffusion and Defect Data Pt.B: Solid State Phenomena, 2006, 116/117: 783−786.

[21] HONG C P, KIM J M. Development of an advanced rheocasting process and its applications [J]. Diffusion and Defect Data Pt.B: Solid State Phenomena, 2006, 116/117: 44−53.

[22] KAUFMANN H, WASBUSSEG H, UGGOWITZER P J. Casting of light metal wrought alloys by new rheocasting [C]//6th International Conference on Semi-Solid Processing of Alloys and Composites. Turin, Italy, 2000: 457−462.

[23] SHANKAR S, SAHA D, APELIAN D, MAKHLOUF M M. CDS: Controlled diffusion solidification: A novel casting approach [C]//8th International Conference on Semi-Solid Processing of Alloys and Composites. Limassol, Cyprus, 2004: Paper 16−2.

[24] LANGLAIS J, LEMIEUX A. The SEED technology for semi-solid processing of aluminum alloys: A metallurgical and process overview [J]. Diffusion and Defect Data Pt.B: Solid State Phenomena, 2006, 116/117: 472−477.

[25] GUO H M, YANG X J. Rheoforging of wrought aluminum alloys [J]. Diffusion and Defect Data Pt.B: Solid State Phenomena, 2008, 141/142/143: 271−276.

[26] KIM D S, KANG C G, LEE S M. Heat treatment processes of A2024 rheoforging alloy and morphology investigation by nanoindentation and atomic force microscopy [J]. Diffusion and Defect Data Pt.B: Solid State Phenomena, 2008, 141/142/143: 385−390.

[27] BAE J W, LEE S M, KANG C G. Forging process of wrought aluminum alloy with controlled solid fraction by electromagnetic stirring [J]. Diffusion and Defect Data Pt.B: Solid State Phenomena,

2008, 141/142/143: 277−282.

[28] MÖLLER H, GOVENDER G, STUMPF W E. The natural and artificial aging response of semi-solid metal processed alloy A356 [J]. Diffusion and Defect Data Pt.B: Solid State Phenomena, 2008, 141/142/143: 737−742.

[29] GOVENDER G, MÖLLER H. Evaluation of surface chemical segregation of semi-solid cast aluminium alloy A356 [J]. Diffusion and Defect Data Pt.B: Solid State Phenomena, 2008, 141/142/143: 433−438.

[30] MÖLLER H, GOVENDER G, STUMPF W E, KNUTSEN R D. Influence of temper condition on microstructure and mechanical properties of semisolid metal processed Al-Si-Mg alloy A356 [J]. International Journal of Cast Metals Research, 2009, 22(6): 417−421.

[31] MÖLLER H, GOVENDER G, STUMPF W E. The T5 heat treatment of semi-solid metal processed aluminium alloy F357 [J]. Materials Science Forum, 2009, 618/619: 365−368.

[32] MASUKU E P, GOVENDER G, IVANCHEV L, MÖLLER H. Rheocasting of Al-Cu alloy A201 with different silver contents [J]. Diffusion and Defect Data Pt.B: Solid State Phenomena, 2008, 141/142/143: 151−156.

[33] CHOU H N, GOVENDER G, IVANCHEV L. Opportunities and challenges for use of SSM forming in the aerospace industry [J]. Diffusion and Defect Data Pt.B: Solid State Phenomena, 2006, 116/117: 92−95.

[34] ALCOA ALLOY 2024 [EB/OL]. http://www.alcoa.com/gcfp/catalog/pdf/alcoa_alloy_2024.pdf.3/18/2010.

[35] ALCOA ALLOY 6082 [EB/OL]. http://www.fairdene.com/chimera/materials%20specs/alloy%206082.pdf.3/18/2010.

[36] ALCOA ALLOY 7075 [EB/OL]. http://www.alcoa.com/gcfp/catalog/pdf/alcoa_alloy_7075.pdf.3/18/2010.

[37] BRUWER R, WILKINS J D, IVANCHEV L H, ROSSOUW P, DAMM O F R A. Method of and apparatus for processing of semi-solid metal alloys: US7368690 [P]. 2008−06−05.

[38] DAVIS J R. Aluminum and aluminum alloys[M]. United States of America: ASM International, 1998: 293.

[39] Standard test methods for tension testing of metallic materials [R]. ASTM E 8M-04.

[40] MÖLLER H, MASUKU E P, CURLE U A. Characterization of surface liquid segregation in SSM-HPDC aluminium alloys 7075, 2024, 6082 and A201 [C]//Proceedings of 11th International Conference on Semi-Solid Processing of Alloys and Composites. Beijing, China, 2010.

[41] MASUKU E P, MÖLLER H, CURLE U A, PISTORIUS P C, LI W. The influence of surface liquid segregation on the corrosion behavior of semi-solid metal high pressure die cast aluminium alloys [C]// Proceedings of 11th International Conference on Semi-Solid Processing of Alloys and Composites. Beijing, China, 2010.

[42] POLMEAR I. Light alloys: From traditional alloys to nanocrystals [M]. 4th Edition. 2006: 57.

[43] MÖLLER H, STUMPF W, PISTORIUS P C. The influence of elevated Fe, Ni and Cr levels on the tensile properties of SSM-HPDC Al-7Si-0.6Mg alloy F357 [C]// Proceedings of 11th International Conference on Semi-Solid Processing of Alloys and Composites. Beijing, China, 2010.

(Edited by YANG Bing)